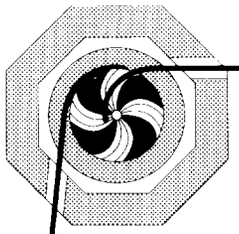

PREPRINT

TASCC-P-94-16

tascc

Multifragment Emission in the 30 A MeV ^{129}Xe + ^{nat}Cu Reaction: A Critical Comparison with Statistical Decay Models

D.R. Bowman[a], N. Colonna[b], W.A. Friedman[c], L. Celano[b], M. D'Agostino[d], J.D. Dinius[e], A. Ferrero[f,1], C.K. Gelbke[e], T. Glasmacher[e], D.O. Handzy[e], D. Horn[a], W.C. Hsi[e], M. Huang[e], I. Iori[f], M.A. Lisa[e,2], W.G. Lynch[e], G.V. Margagliotti[g], P.M. Milazzo[d], C.P. Montoya[e], A. Moroni[f], G.F. Peaslee[e,3], L. Phair[e,2], F. Petruzzelli[f], R. Scardaoni[f], C. Schwarz[e,4], M.B. Tsang[e], and C. Williams[e]

[a]AECL Research, Chalk River Laboratories, Chalk River, Ontario, Canada K0J 1J0
[b]INFN, Via Amendola 173, 70126 Bari, Italy
[c]Department of Physics, University of Wisconsin, Madison, Wisconsin 53706, USA
[d]Dipartimento di Fisica and INFN, Via Irnerio 46, 40126 Bologna, Italy
[e]NSCL, Michigan State University, E. Lansing, Michigan 48824, USA
[f]Dipartimento di Fisica and INFN, Via Celoria 12, 20133 Milano, Italy
[g]Dipartimento di Fisica and INFN, Via A. Valerio 2, 34127 Trieste, Italy

[1] On leave from the Comisión de Energia Atómica, Argentina
[2]Present address: Lawrence Berkeley Laboratory, 1 Cyclotron Rd., Berkeley, CA 94720, USA
[3]Present address: Physics Department, Hope College, Holland, MI 49223, USA
[4]Present address: Gesellschaft für Schwerionenforschung, D-6100 Darmstadt, Germany

Submitted to Phys. Lett. B.

NOTICE

Physical and Environmental Sciences
Chalk River Laboratories
Chalk River, ON K0J 1J0 Canada

1994 August

Multifragment Emission in the 30 A MeV ^{129}Xe + ^{nat}Cu Reaction: A Critical Comparison with Statistical Decay Models

D.R. Bowman[a], N. Colonna[b], W.A. Friedman[c], L. Celano[b], M. D'Agostino[d], J.D. Dinius[e], A. Ferrero[f,1], C.K. Gelbke[e], T. Glasmacher[e], D.O. Handzy[e], D. Horn[a], W.C. Hsi[e], M. Huang[e], I. Iori[f], M.A. Lisa[e,2], W.G. Lynch[e], G.V. Margagliotti[g], P.M. Milazzo[d], C.P. Montoya[e], A. Moroni[f], G.F. Peaslee[e,3], L. Phair[e,2], F. Petruzzelli[f], R. Scardaoni[f], C. Schwarz[e,4], M.B. Tsang[e], and C. Williams[e]

[a] *AECL Research, Chalk River Laboratories, Chalk River, Ontario, Canada K0J 1J0*
[b] *INFN, Via Amendola 173, 70126 Bari, Italy*
[c] *Department of Physics, University of Wisconsin, Madison, Wisconsin 53706, USA*
[d] *Dipartimento di Fisica and INFN, Via Irnerio 46, 40126 Bologna, Italy*
[e] *NSCL, Michigan State University, E. Lansing, Michigan 48824, USA*
[f] *Dipartimento di Fisica and INFN, Via Celoria 12, 20133 Milano, Italy*
[g] *Dipartimento di Fisica and INFN, Via A. Valerio 2, 34127 Trieste, Italy*

ABSTRACT

Multifragment emission has been studied in central 30 A MeV ^{129}Xe + ^{nat}Cu reactions and compared with predictions of schematic three-body trajectory calculations and with three different statistical decay models. The trajectory calculations indicate a mean fragment emission time of $\approx$ 200 fm/c, consistent with fast, sequential decay. The statistical models that allow expansion provide agreement with the measured fragment multiplicities, but none of the models is able to simultaneously reproduce the fragment-fragment relative-velocity correlations and the fragment emission velocities.

Typeset using REVTEX

[1]On leave from the Comisión de Energia Atómica, Argentina

[2]Present address: Lawrence Berkeley Laboratory, 1 Cyclotron Rd., Berkeley, CA 94720, USA

[3]Present address: Physics Department, Hope College, Holland, MI 49223, USA

[4]Present address: Gesellschaft für Schwerionenforschung, D-6100 Darmstadt, Germany

An understanding of multifragment emission (Z > 2) during heavy-ion collisions [1] can provide important information about the properties of excited nuclear matter, such as its compressibility at low density and the possibility of a liquid-gas phase transition [2]. Comparisons of experimental data with model predictions have indicated that nuclear expansion is needed to reproduce the observed fragment multiplicities [3–5] and charge distributions [6]. However, other issues sensitive to the possibility of a phase transition, such as the space-time extent of the fragmenting system [7–15], and decay via surface or volume emission [16], have not been systematically compared with realistic models.

In this paper we examine three properties of multifragment decay in the 30 A MeV ^{129}Xe + ^{nat}Cu reaction: the average fragment multiplicity, the fragment-fragment reduced-velocity correlation function, and the average emission velocity of fragments with Z=6. We compare the data with predictions of three statistical-decay models with initial conditions based upon a microscopic transport-model calculation.

A 30 A MeV ^{129}Xe beam delivered by the K1200 Cyclotron at Michigan State University impinged upon targets of ^{nat}Cu of 2 mg/cm^2 areal density. Charged reaction products were measured between 23° and 160 ° with 158 elements (Rings 3-11) of the MSU Miniball [17]. Fragments emitted at more forward angles, 8° - 23° were detected with 36 elements of the high-resolution gas-Si-Si(Li)-CsI MULTICS array [18]. Identification thresholds were approximately E/A = 2, 3, and 4 MeV for Z = 3, 10, and 18 fragments in the Miniball; and approximately E/A = 1.5 MeV for fragments of all atomic numbers in the MULTICS array. Energy resolutions of $\approx$ 10%, and better than 2% were obtained with the Miniball, and the MULTICS detectors, respectively; and an angular resolution of $\approx$ 0.2 ° was obtained with the MULTICS array. The total detector system covered a solid angle of > 87% of 4π.

The measured charged-particle multiplicity (N_C) distribution shows a broad, flat region extending to multiplicities of approximately 13 and a sharply falling tail at larger multiplicities. In this paper, we will concentrate on the most violent events with $N_C > 13$, which

correspond to the upper 14% of the distribution of detected events ($N_C \geq 2$). For these events the average number of detected intermediate mass fragments (IMF: $3 \leq Z \leq 20$) is 1.7, and is nearly independent of N_C.

We have compared the experimental data with calculations of three statistical-decay models with varying assumptions about the space-time characteristics of the fragmenting system. The model GEMINI [19] calculates sequential binary emission of all species ranging from nucleons to symmetric fission fragments. Each decay product is assumed to be fully accelerated by the Coulomb field of its partner before the succeeding particle or fragment is emitted. The Expanding-Emitting Source Model (EES) of Friedman [20] treats surface emission of light particles and fragments ($Z \leq 9$) assuming binary phase space. Dynamics are built into the model to allow both fragment emission and expansion or contraction of the source as a function of time. The Berlin Multifragmentation Model (BMM) [21] calculates the simultaneous disassembly of an expanded nuclear system characterized by a freeze-out radius of $r_{FO} = r_0 A^{1/3}$, typically with $r_0 \geq 2.1$ fm.

In order to estimate the properties of an equilibrated source, we have used the BNV model of ref. [22] to simulate the early dynamical stage of the collision. Calculations at an impact parameter of b=0 were followed to times of 140 fm/c [23]. The source properties for GEMINI and the EES model were determined at a time following compression when the nuclear matter returns to normal density ($\approx$80 fm/c). Since these models assume spherical symmetry, a radial decomposition of the matter distribution predicted by the BNV model was performed [24]. Two sets of input parameters were extracted: the first assuming a source radius of r_S=9 fm, and the second assuming a source radius of r_S=8 fm. The charge, mass, thermal excitation energy, and energy of radial expansion were used as input into the EES calculations. Only a single set of input parameters was used in the GEMINI calculations corresponding to the higher excitation energy case, r_S=9 fm. Because GEMINI does not allow expansion, the excitation energy was taken to be the sum of the thermal and radial expansion energies. A triangular angular momentum distribution between 0 and 70 $\hbar$ was used in GEMINI. [25].

The BMM assumes nuclear disintegration at low density. Therefore, the coupling with the dynamical calculation was chosen to be at the point of maximum expansion (t=115 fm/c, ρ/ρ_0=0.6) [26]. Two calculations were performed with the BMM model: the first with a standard radius parameter of 2.1 fm (r_{FO}=11.8 fm) and the second with an extended radius parameter of 2.6 fm (r_{FO}=14.6 fm). The values of the parameters used in the statistical model calculations are listed in Table 1.

The calculated and filtered average IMF multiplicities are also shown in Table 1. The two EES calculations bracket the measured value of 1.7, the BMM calculations slightly overpredict the data, and the GEMINI calculation strongly underpredicts the data. EES calculations that do not allow expansion, shown in parentheses, are significantly smaller than the data. These results suggest that expansion may be important even at the rather low bombarding energy of 30 A MeV.

Determination of the fragment emission time scale may provide further information about the disassembly mechanism. In order to obtain a quantitative measure of this time scale we have compared the experimental two-fragment ($4 \leq Z \leq 9$) reduced-velocity correlation function [7–13] with schematic, three-body trajectory calculations described in ref. [27]. The experimental energy and angular distributions measured with the high-resolution MULTICS array were used in the trajectory calculations, and the uncorrelated distribution was constructed with the event-mixing technique [28]. In Fig. 1, the data are compared with calculations assuming a source radius of r_S=12 fm, and various mean emission times ranging from 0 to 500 fm/c. Best agreement is obtained with an emission time of τ=200 fm/c (solid curve). To quantify the level of agreement, a contour plot of the reduced chi-squared values in τ-r_S space is shown as an inset in the figure [29]. For all assumed source radii between 8 and 14 fm, a time scale of 200 fm/c gives the best agreement with the data. This emission time scale is fast, but is consistent with that of sequential decay. For orientation, a ^{12}C fragment with an energy of 13 MeV (approximately twice the temperature of the system of interest) will travel a distance corresponding to $\approx$ 1.75 times its diameter in a time of 200 fm/c.

The measured mean fragment emission time can be directly compared with the EES calculations. Mean emission times of ~190 fm/c and ~110 fm/c were calculated for the two cases with source radii of 8 fm, and 9 fm, respectively. The mean emission time for the r_S=8 fm case, determined solely from the input parameters provided by the BNV calculations, agrees quantitatively with the experimental emission time determined from the trajectory calculations.

In Figure 2 the experimental correlation function is compared with filtered calculations generated by the three statistical decay models. For the GEMINI and BMM calculations the raw N-body event files were passed through a software replica of the MULTICS array. For the EES calculations the three-body trajectory code described above was modified to generate correlation functions based on the theoretical charge distributions, emission time distributions, and the (time-dependent) source charge, mass, temperature and radius. These calculated events were then passed through the experimental filter. In the top panel the correlation functions based upon the r_S=8 fm (dashed curve) and r_S=9 fm (dotted curve) EES calculations are shown. Although the calculated emission times agree well with those determined from the trajectory calculations, the correlation functions exhibit differences. Because the angular distributions assumed in the EES model do not correspond to the experimental angular distributions, the initial positioning of the fragments in the EES and trajectory calculations differs [30]. Using the experimental angular distributions rather than the isotropic angular distributions predicted by the EES model leads to the correlation functions shown by the solid (r_S=8 fm) and dot-dashed (r_S=9 fm) curves. The agreement of these calculations with the data is much improved, demonstrating that realistic single-particle distributions must be used for quantitative analyses of correlation functions.

The bottom panel of Figure 2 shows the correlation functions predicted by GEMINI and the BMM model. The GEMINI calculation (dotted curve) gives a completely incorrect shape. Approximately one-half of the coincident fragment-fragment pairs generated by GEMINI are formed by the binary splitting of a primary parent. This process gives rise to a well-defined relative velocity between the two IMFs and a strong peak in the correlation

function that is not observed in the data. The BMM calculation with the standard freeze-out radius of 11.8 fm also gives poor agreement with the data. Better agreement can be obtained with a larger radius of 14.6 fm. However, because of the dual sensitivity of the correlation function to space and time such a large radius may be unrealistic and mimic a finite lifetime that is not considered in the BMM model. To determine if simultaneous fragment emission from a greatly-expanded system is realistic, we examine the emission velocities predicted by the different decay models.

The centroid (standard deviation) of the experimental source velocity distribution for $N_C > 13$ events was determined to be 0.174 c (0.015 c) by the coincident-fragment source-velocity technique developed in ref. [31]. This average source velocity corresponds to nearly full (92%) momentum transfer in the simple incomplete-fusion model. The experimental data were transformed event-by-event into this source frame. The solid and open points in Fig. 3 show the centroid and standard deviation of the experimental emission velocity distributions for Z=6 fragments as a function of emission angle in this frame. The nearly constant values of V_{Emiss} over the range of θ_{Source}=35°-115° are consistent with equilibrium emission. The larger values of V_{Emiss} at small θ_{Source} are caused by the experimental acceptance. The slow increase at larger θ_{Source} presumably indicates an additional nonequilibrium component of fragment emission that persists even in the most violent events with $N_C > 13$ [13].

After folding over the experimental source velocity distribution, the calculated centroids and standard deviations of the Z=6 emission velocity distributions are shown in Fig. 3. Both of the EES calculations overpredict the average emission velocity in the θ_{Source} range where equilibrium emission dominates. The GEMINI calculation shows good agreement with the data. This better agreement is likely a consequence of GEMINI calculating emission velocities based upon empirical systematics and allowing sequential decays of excited primary fragments. The BMM calculation with a freeze-out radius of 11.8 fm underpredicts, and that with a freeze-out radius of 14.6 fm greatly underpredicts the average emission velocities. The smaller velocities predicted by the calculation with the larger radius are because of the smaller Coulomb energy of the system. This underprediction indicates that the simultaneous

decay of a greatly-expanded source is an unrealistic assumption, unless a collective radial velocity (not treated in the BMM) is included.

In summary, comparisons with three-body trajectory calculations indicate a mean fragment emission time of $\approx$200 fm/c consistent with a fast, but nevertheless sequential, time scale. GEMINI calculations drastically underpredict the fragment multiplicity and give a completely incorrect correlation function because of the large number of primary fragments decaying into coincident IMFs. In contrast, the models which allow expansion either explicitly (EES) or implicitly (BMM) are able to reproduce the average fragment multiplicity. The EES model predicts an approximately correct mean fragment emission time, as determined by the trajectory calculations, but the correlation function and the fragment emission velocities are not well reproduced. Use of the experimental angular distributions significantly improves the agreement with the experimental correlation functions. Varying the radius parameter in the BMM model can provide agreement with either the correlation function (large radius simulating a finite lifetime) or with the fragment emission velocities (standard radius), but not with both simultaneously. These results illustrate the need to reproduce single-particle observables together with more complex quantities.

This work was supported by the National Science Foundation under Grants PHY-90-15255 and PHY-92-14992.

REFERENCES

[1] For an overview of this process, see L.G. Moretto and G.J. Wozniak, Annu. Rev. Nucl. Part. Sci. 43 (1993) 379.

[2] P.J. Siemens, Nature 305 (1983) 410.

[3] D.R. Bowman et al., Phys. Rev. Lett. 67 (1991) 1527.

[4] R.T. de Souza et al., Phys. Lett. B 268 (1991) 6.

[5] J. Hubele et al., Phys. Rev. C 46 (1992) R1577.

[6] K. Hagel et al., Phys. Rev. Lett. 68 (1992) 2141.

[7] Y.D. Kim et al., Phys. Rev. C 45 (1992) 338.

[8] D. Fox et al., Phys. Rev. C 47 (1993) R421.

[9] D.R. Bowman et al., Phys. Rev. Lett. 70 (1993) 3534.

[10] E. Bauge et al., Phys. Rev. Lett. 70 (1993) 3705.

[11] T.C. Sangster et al., Phys. Rev. C 47 (1993) R2457.

[12] B. Kämpfer et al., Phys. Rev. C 48 (1993) R955.

[13] O. Lopez et al., Phys. Lett. B 315 (1994) 34.

[14] O. Schapiro, A.R. DeAngelis, and D.H.E. Gross, Nucl. Phys. A 568 (1994) 333.

[15] O. Schapiro and D.H.E. Gross, Nucl. Phys. A 573 (1994) 143.

[16] R.T. de Souza et al., Phys. Lett. B 300 (1993) 29.

[17] R.T. de Souza et al., Nucl. Instr. Meth. A 295 (1990) 109.

[18] I. Iori et al., Nucl. Instr. Meth. A 325 (1993) 458.

[19] R.J. Charity et al., Nucl. Phys. A 483 (1988) 371.

[20] W.A. Friedman, Phys. Rev. Lett. 60 (1988) 2125; a finite-nucleus compressibility of 144 MeV was used in the calculations.

[21] D.H.E. Gross, Rep. Prog. Phys. 53 (1990) 605.

[22] A. Bonasera et al., Phys. Lett. B 221 (1989) 233. The standard compressibility of K = 200 MeV was used in these calculations.

[23] At t=0 the projectile and target surfaces are separated by approximately 2 fm.

[24] D.R. Bowman et al., Phys. Rev. C 46 (1992) 1834.

[25] An angular momentum of 70 $\hbar$ is the maximum the source can sustain with a non-zero fission barrier. BNV calculations at b = 4 fm (the impact parameter bounding the most central 14% of the geometric cross section) give angular momenta greater than 70 $\hbar$.

[26] M. Colonna et al, Phys. Lett. B 283 (1992) 180.

[27] T. Glasmacher et al., preprint MSUCL-923 and submitted to Phys. Rev. C. The code described herein reproduces the calculations of refs. [7-9].

[28] A source charge of Z_S=77 was used in the calculations. The low energy portion of the energy distribution was not sampled because of the schematic nature of the simulatations (See details in ref. [27]). However, the rising part of the angle-integrated correlation functions is quite insensitive to the exact nature of the energy distribution sampled. This was verified by performing additional calculations with Z_S = 25, 40, and 50.

[29] A total area normalization of the numerator to the denominator was used as suggested in ref. [14,15]. The chi-squared values were determined over the rising portion of the correlation function, v_{red} = 0.004 c - 0.017 c.

[30] The initial positioning of the fragments was performed assuming Lambert's law for surface emission. See ref. [7].

[31] N. Colonna et al., Phys. Rev. Lett. 62 (1989) 1833; a total detected charge of at least

35 was required for each event in the source velocity distribution.

FIGURES

FIG. 1. Comparison of experimental fragment-fragment reduced-velocity correlation functions (solid points) with three-body trajectory calculations (curves). The calculations were performed assuming a source radius, r_S, of 12 fm and the indicated mean emission times, τ. Inset: Contours of chi-squared per degree of freedom for three-body trajectory calculations in τ - r_S space. Solid contours correspond to levels of 10, 40, and 160. Dotted contours correspond to levels of 20 and 80.

FIG. 2. Comparison of experimental correlation functions (solid points) with filtered statistical model calculations. Top: EES with r_S=8 fm and experimental angular distribution (solid curve), r_S=9 fm and experimental angular distribution (dot-dashed curve), r_S=8 fm (dashed curve), and r_S=9 fm (dotted curve). Bottom: BMM with r_S=14.6 fm (solid curve), BMM with r_S=11.8 fm (dashed curve), and GEMINI (dotted curve).

FIG. 3. The first (solid points) and second (open points) moments of the emission velocity distributions in the source frame (V_S=0.174 c) as a function of emission angle. The curves correspond to filtered calculations with the indicated statistical models.

TABLES

TABLE I. Parameters for statistical models calculations: time of the coupling, source (freeze-out) radius, charge, mass, excitation energy, and energy of radial expansion; and the mean fragment multiplicities calculated with each model.

	τ (fm/c)	r (fm)	Z	A	E* (MeV)	E_R (MeV)	$<N_{IMF}>$
GEMINI	80	9	77	175	860	-	0.36
EES	80	9	77	175	700	160	1.99 (0.82)
EES	80	8	73	165	540	130	1.11 (0.65)
BMM	115	14.6	76	177	750	-	2.38
BMM	115	11.8	76	177	750	-	2.29

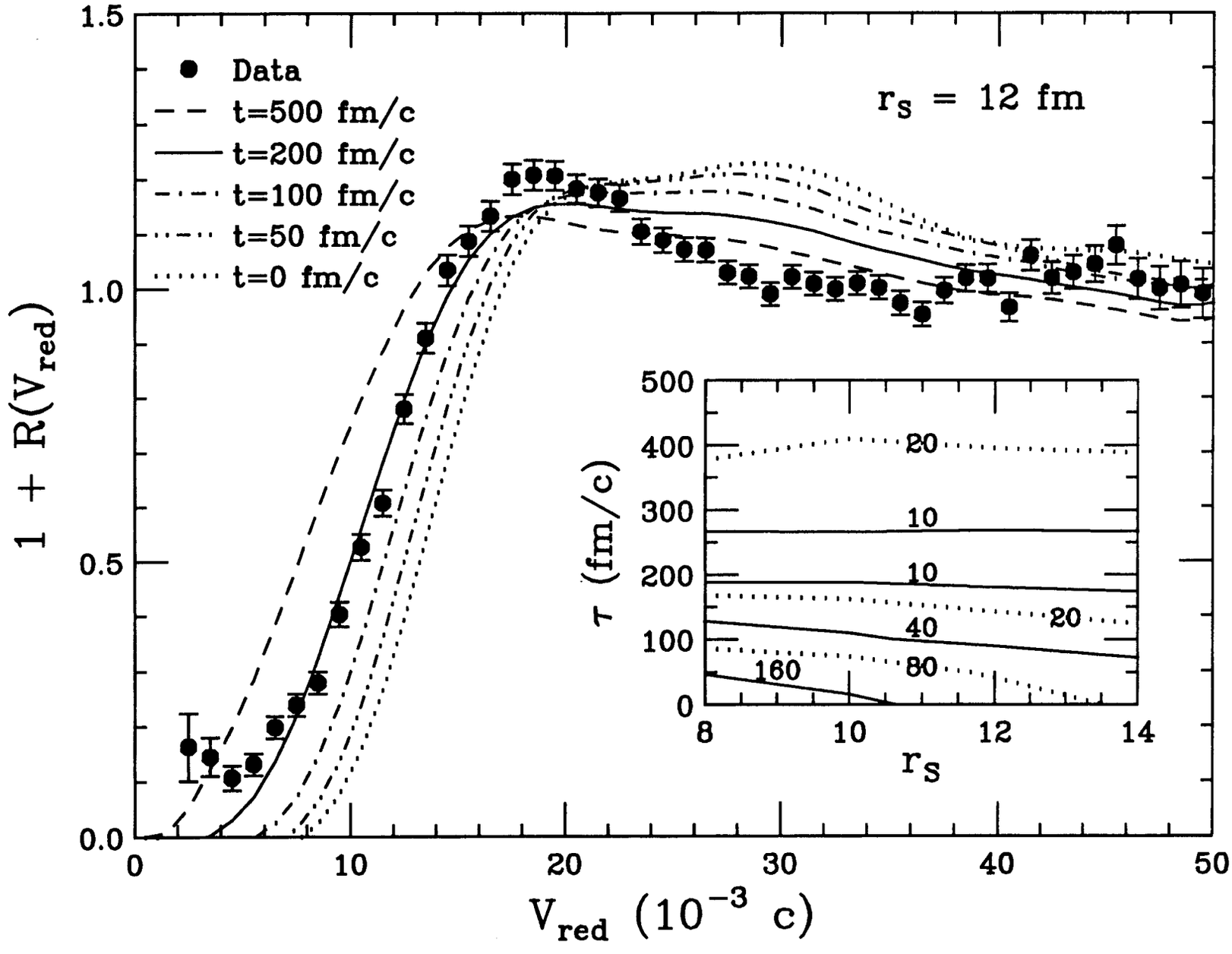
Data
t=500 fm/c
t=200 fm/c
t=100 fm/c
t=50 fm/c
t=0 fm/c
r_s = 12 fm
$1 + R(V_{red})$
V_{red} (10^{-3} c)
τ (fm/c)
r_s
20
10
10
40
20
160
80

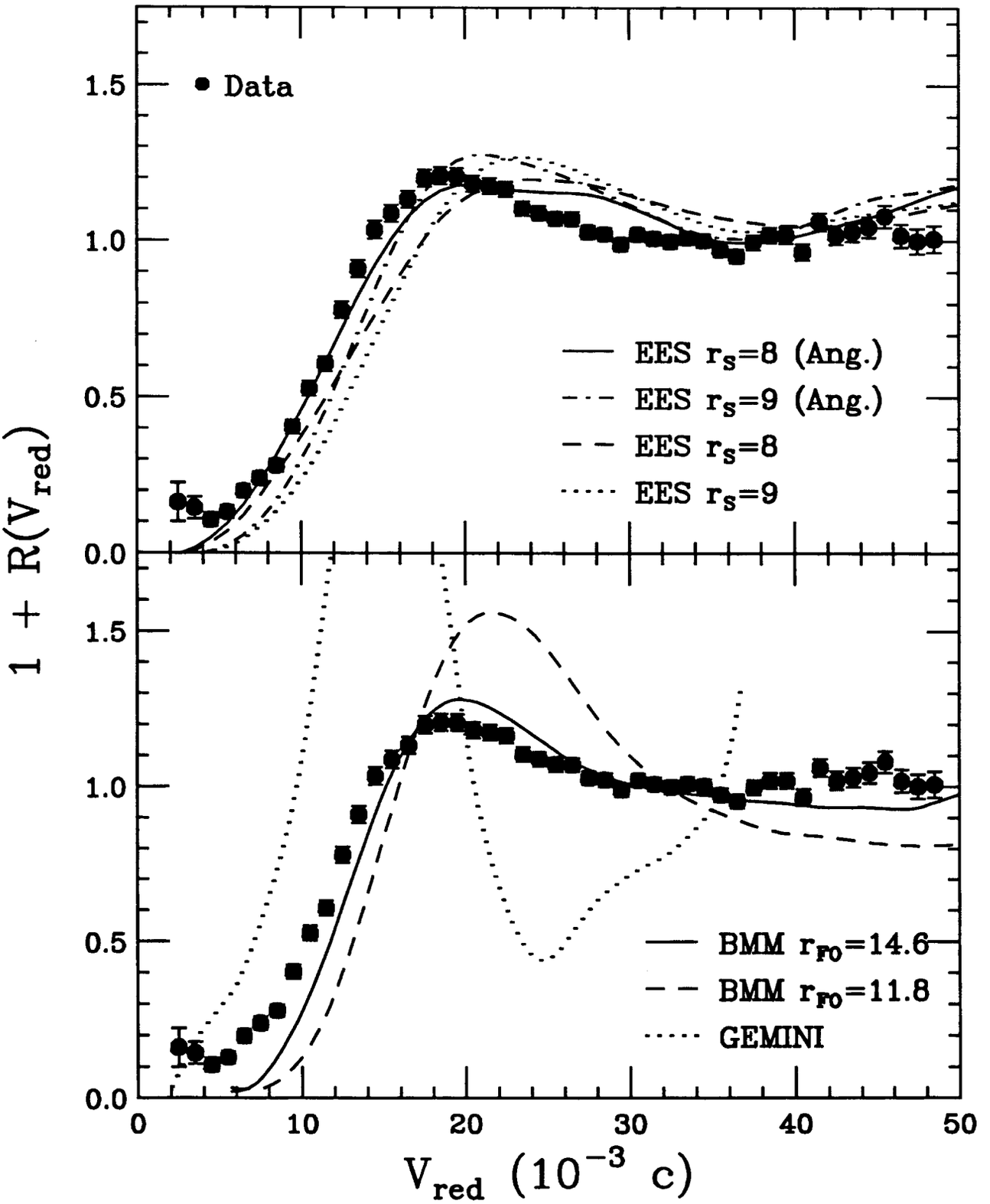
Data
EES r_s=8 (Ang.)
EES r_s=9 (Ang.)
EES r_s=8
EES r_s=9
BMM r_{FO}=14.6
BMM r_{FO}=11.8
GEMINI
1 + R(V_{red})
V_{red} (10^{-3} c)
0.0
0.5
1.0
1.5
0
10
20
30
40
50

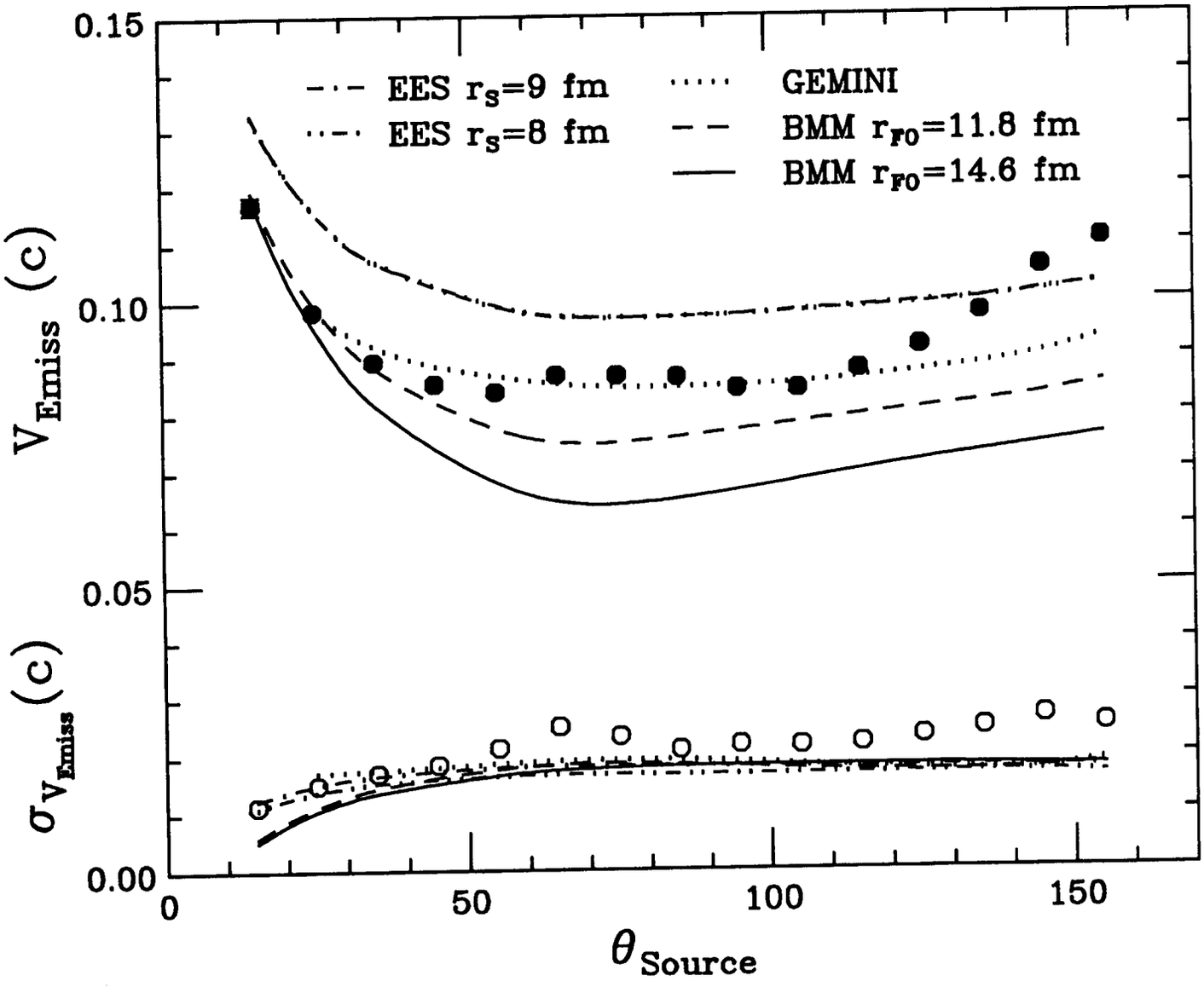
0.15
0.10
0.05
0.00
0
50
100
150
EES r_s=9 fm
EES r_s=8 fm
GEMINI
BMM r_{FO}=11.8 fm
BMM r_{FO}=14.6 fm
V_{Emiss} (c)
$\sigma_{V_{Emiss}}$ (c)
θ_{Source}